Spin-Stretching Modes in Anisotropic Magnets: Spin-Wave Excitations in the Multiferroic $Ba_2CoGe_2O_7$

K. Penc,[1,2] J. Romhányi,[1,2] T. Rõõm,[3] U. Nagel,[3] Á. Antal,[2] T. Fehér,[2] A. Jánossy,[2] H. Engelkamp,[4] H. Murakawa,[5,6] Y. Tokura,[5,6,7,8] D. Szaller,[2] S. Bordács,[2,5,6] and I. Kézsmárki[2,5]

[1]*Institute for Solid State Physics and Optics, Wigner Research Centre for Physics, Hungarian Academy of Sciences, H-1525 Budapest, P.O.B. 49, Hungary*

[2]*Department of Physics, Budapest University of Technology and Economics and Condensed Matter Research Group of the Hungarian Academy of Sciences, 1111 Budapest, Hungary*

[3]*National Institute of Chemical Physics and Biophysics, 12618 Tallinn, Estonia*

[4]*High Field Magnet Laboratory, Institute for Molecules and Materials, Radboud University, 6525 ED Nijmegen, The Netherlands*

[5]*Multiferroics Project, ERATO, Japan Science and Technology Agency (JST), Japan c/o The University of Tokyo, Tokyo 113-8656, Japan*

[6]*Quantum-Phase Electronics Center, Department of Applied Physics, The University of Tokyo, Tokyo 113-8656, Japan*

[7]*Department of Applied Physics, The University of Tokyo, Tokyo 113-8656, Japan*

[8]*Cross-Correlated Materials Group (CMRG) and Correlation Electron Research Group (CERG), RIKEN Advanced Science Institute, Wako 351-0198, Japan*

(Received 13 March 2012; published 19 June 2012)

We studied spin excitations in the magnetically ordered phase of the noncentrosymmetric $Ba_2CoGe_2O_7$ in high magnetic fields up to 33 T. In the electron spin resonance and far infrared absorption spectra we found several spin excitations beyond the two conventional magnon modes expected for such a two-sublattice antiferromagnet. We show that a multiboson spin-wave theory describes these unconventional modes, including spin-stretching modes, characterized by an oscillating magnetic dipole and quadrupole moment. The lack of inversion symmetry allows each mode to become electric dipole active. We expect that the spin-stretching modes can be generally observed in inelastic neutron scattering and light absorption experiments in a broad class of ordered $S > 1/2$ spin systems with strong single-ion anisotropy and/or noncentrosymmetric lattice structure.

DOI: 10.1103/PhysRevLett.108.257203 PACS numbers: 75.85.+t, 75.10.−b, 75.30.Gw, 76.50.+g

Magnons are collective spin excitations in crystals with long-range magnetic order, often investigated by electromagnetic absorption and inelastic neutron scattering (INS) experiments. Both classical and quantum spin-wave theory of $S = 1/2$ systems predict one magnon branch in the spin excitation spectrum for each spin in the magnetic unit cell [1]. This rule about the number of magnon branches is generally accepted and experimentally verified for $S > 1/2$ spin systems as long as the conventional spin-wave theory applies, requiring that the lengths (in other words, the absolute values of the expectation values) of the spins are preserved in the excited states and only their orientations change relative to the ground state configuration [2]. However, the picture of one magnon mode per spin in the magnetic unit cell needed to be surpassed in several f-electron compounds with complicated quadrupolar ordering, such as CeB_6 [3] and UO_2 [4].

Recently, additional spin-wave modes have been observed by far infrared (FIR) spectroscopy [5] and INS [6] in $Ba_2CoGe_2O_7$, a simple two sublattice spin-3/2 easy-plane antiferromagnet (AF) below $T_{\mathrm{Néel}} = 6.7$ K [7,8]. This material has attracted much interest owing to its multiferroic ground state where delicate magnetic control of the ferroelectric polarization [8,9] and chirality [10] were realized. Moreover, spin waves in $Ba_2CoGe_2O_7$ exhibit giant directional dichroism and natural optical activity at THz frequencies due to the large ac magnetoelectric effect [5,10]. A recent numerical diagonalization study on finite spin clusters found, besides the two conventional AF modes, additional spin resonances with peculiar optical properties [10,11]. Nevertheless, the understanding of the unconventional magnon modes and the coupled dynamics of spins and electronic polarization on a fundamental level remained an open issue.

In this Letter, we investigate the spin-wave excitations in $Ba_2CoGe_2O_7$ over a broad photon energy range combining electron spin resonance (ESR) and high-resolution FIR spectroscopy. The largest magnetic field, 33 T, applied in this study drastically changes the antiferromagnetic spin configuration for any field direction, in contrast to former experiments restricted to $B_{\mathrm{dc}} \leq 12$ T. The orientation of B_{dc} and the light polarization relative to the main crystallographic axes were systematically varied in order to map the field dependence and the selection rules of the modes. We derive a multiboson spin-wave theory and show that a large single-ion anisotropy plays a key role in the emergence of new magnetic excitations involving the oscillation of spin length, and that the lack of inversion symmetry, a necessary condition for the dc and ac magnetoelectric effects, renders these spin waves electric dipole active.

$Ba_2CoGe_2O_7$ has a noncentrosymmetric tetragonal space group, $P\bar{4}2_1m$. The magnetic Co^{2+} ions are surrounded by tetrahedra of oxygens compressed along the [001] tetragonal axis. Due to the lack of inversion symmetry, a coupling between spins and local polarization appears [12,13]. This was observed as a magnetic order induced ferroelectricity in this family of materials including $Ba_2CuGe_2O_7$ [8,9], $Ca_xSr_{2-x}CoSi_2O_7$ [14], and $Ba_2MnGe_2O_7$ [15].

Here we study spin-wave resonances in the magnetic phase of $Ba_2CoGe_2O_7$ on high-quality single crystals at temperatures between 1.8 and 4 K; in this range the excitation spectrum hardly changes. ESR spectroscopy was performed at 75, 111, 150, and 222 GHz using solid state oscillators, while FIR transmission was measured by Fourier transform spectroscopy over the region of 0.15–2 THz (0.6–8 meV) with a resolution of 15 GHz.

An overview of the spectra for representative directions of the magnetic field is given in Fig. 1. Two sharp peaks are present in the zero field FIR absorption spectra at $f \sim 0.5$ and 1 THz, in accordance with former studies [5,10]. The first is assigned to the usual optical magnon branch gapped by magnetic anisotropy of mostly single-ion origin. The second is not captured by conventional spin-wave theory, and was shown to respond to both the magnetic and electric component of light and termed as an electromagnon [5]. For B_{dc} along the tetragonal axis, as in Figs. 1(a) and 1(c), the 1 THz mode shows a V shape splitting with a double-peak structure on the high-energy side. The double-peak structure is clearly visible when $E_\omega \parallel [010]$ [see Fig. 1(c)]. The frequency of the 0.5 THz mode slightly increases in low fields [Figs. 1(a) and 1(c)]; however, it turns back after an avoided crossing with the lower branch of the 1 THz resonance at $B_{dc} \approx 12$ T.

The rotation of B_{dc} from the tetragonal axis to the tetragonal plane affects all the modes drastically (Fig. 1). For $B_{dc} \parallel [100]$, the 1 THz mode is again split into three distinct lines. However, they exhibit only a weak softening up to a kink at $B_{dc} \approx 16$ T, from where the resonance frequencies start to increase quickly [Fig. 1(b)]. The magnon mode at $f \sim 0.5$ THz becomes silent with increasing field for both polarization directions in the Faraday geometry ($\mathbf{k} \| B_{dc}$).

An additional low frequency mode appears in the ESR and FIR spectra when B_{dc} is within the tetragonal plane, breaking the fourfold rotoinversion symmetry of the lattice. This mode corresponds to the quasi Goldstone mode of an easy-plane AF when $B_{dc} = 0$. The frequency of this

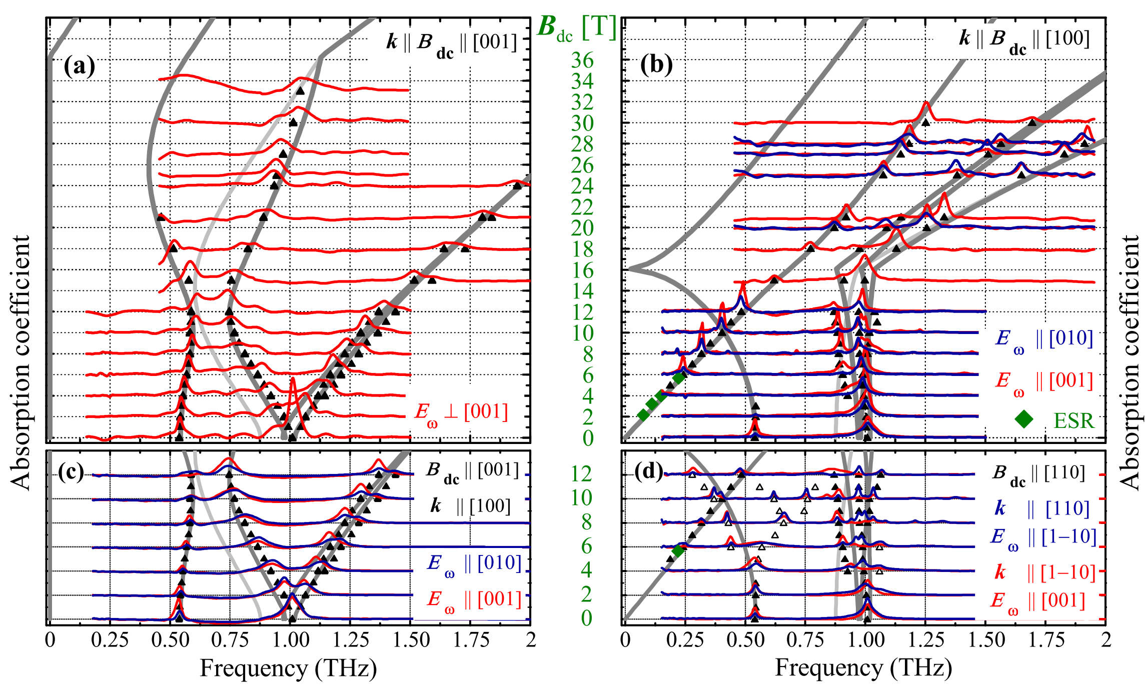

FIG. 1 (color online). Magnetic field dependence of the absorption spectra in $Ba_2CoGe_2O_7$ below 2 THz for a representative set of light polarizations. The spectra are shifted vertically proportional to the magnitude of the field, B_{dc}. The separation between horizontal grid lines corresponds to an absorption coefficient of 20 cm^{-1} in panels (a) and (c), and 30 cm^{-1} in (b) and (d). The direction of B_{dc} is indicated in each panel and the spectra for different polarizations and propagation directions ($\mathbf{k}$) of light are distinguished by the color. Black triangles and green diamonds represent the position of the resonances determined from the FIR and ESR spectra, respectively. Below 12 T the triangles are shown in 1 T steps, while the spectra are displayed only in 2 T steps for clarity. The gray lines show the field dependence of the modes obtained in our multiboson spin-wave approach. (d) For $B_{dc} \perp [001]$ in some polarization configurations, two of which are shown, we observed additional modes (open triangles) not explained by the theory.

mode is not affected measurably by the orientation of B_{dc} in the plane and follows a linear field dependence down to 75 GHz. Hence, the in-plane anisotropy gap is significantly less than 75 GHz.

If B_{dc} is in the tetragonal plane, the number of observed resonances exceeds six in some polarization configurations. Two representative cases are presented in Fig. 1(d). The 0.5 THz mode suddenly splits into a sharp and a broad feature at $B_{dc} = 5$ T, while the 1 THz branch consists of at least four resonances. At $\gtrsim 12$ T, the number of modes is reduced.

As a microscopic model, we consider the Hamiltonian below to describe the $S = 3/2$ spin Co^{2+} ions. Following Ref. [11], we have a large single-ion anisotropy Λ, but we introduce an anisotropic exchange coupling (J and J_z) and neglect the Dzyaloshinskii-Moriya term that appeared to have negligible effect on the excitations,

$$\mathcal{H} = J\sum_{\langle i,j\rangle}(S_i^x S_j^x + S_i^y S_j^y) + J_z\sum_{\langle i,j\rangle}S_i^z S_j^z + \sum_i[\Lambda(S_i^z)^2 + g_{zz}h_z S_i^z + g_{xx}(h_x S_i^x + h_y S_i^y)], \quad (1)$$

where $\langle i, j\rangle$ indicates nearest neighbor pairs, and the x, y, and z axes are parallel to the [110], [$1\bar{1}0$], and [001] crystallographic directions, respectively. $g_{xx} = g_{yy}$ and g_{zz} are the principal values of the g tensor, and $h_\alpha = \mu_B B_{dc,\alpha}$ are the components of the magnetic field.

We assume a site factorized variational wave function $|\Psi_0\rangle = \prod_{i\in A}|\Psi_A(i)\rangle\prod_{i\in B}|\Psi_B(i)\rangle$ to describe the long-range ordered ground state of the system of two spin sublattices A and B (i is the site index). For example, when $B_{dc} \parallel [110]$ and $J_z/J \lesssim 4$, we get a canted Néel state [16] where the expectation values of spin components are

$$\langle\Psi_X(i)|\hat{\mathbf{S}}_X|\Psi_X(i)\rangle = \frac{3\eta(\eta+1)}{3\eta^2+1}(\cos\varphi_X, \sin\varphi_X, 0). \quad (2)$$

The two variational parameters η and $\varphi_A = -\varphi_B$ are determined from the minimization of the energy ($X = A, B$). We note that $\eta \neq 1$ corresponds to a spin with length smaller than 3/2, the consequence of the on-site anisotropy.

This $|\Psi_0\rangle$ serves as a starting point to study excitations: we introduce four orthogonal bosons on each site, denoted by $a^\dagger_{\nu,X}(i)$, where $\nu = 0, \ldots, 3$, so that the variational ground state is $|\Psi_X(i)\rangle = a^\dagger_{0,X}(i)|\text{vacuum}\rangle$. Any product of the operators on a site can be expressed as a quadratic form of the four a bosons and they satisfying the expected commutation relations. The number of bosons on each site is conserved, $\sum_{\nu=0}^3 a^\dagger_{\nu,X}a_{\nu,X} = M$, and $M = 1$ for the $S = 3/2$ spin. The linear multiboson spin-wave theory is a $1/M$ expansion, where the $a^\dagger_{\nu,A}$ and $a^\dagger_{\nu,B}$ with $\nu = 1, 2, 3$ play the role of the Holstein-Primakoff bosons and describe the excitations, the generalized spin waves. Replacing $a^\dagger_{0,X}$ and $a_{0,X}$ with $(M - \sum_{\nu=1}^3 a^\dagger_{\nu,X}a_{\nu,X})^{1/2}$ and performing the expansion in $1/M$ one can follow the procedure of the conventional spin-wave theory, and we get a Hamiltonian that is quadratic in boson operators and straightforward to diagonalize (see Supplemental Material [17]). A similar approach has been used to describe, for example, CeB_6 [3], the SU(4) Heisenberg model [18], the $TlCuCl_3$ a spin ladder [19], and multipolar excitations in the spin-1 [20] and spin-3/2 [21] Heisenberg models.

The spectrum as a function of Λ/J in zero magnetic field and for zero momentum is shown in Fig. 2(a). It consists of six modes, three for each Co spin in the unit cell. A finite anisotropy reduces the O(3) symmetry of the Hamiltonian to O(2), decreasing the number of zero energy Goldstone modes from two to one.

Let us begin from $\Lambda = 0$. Then $\eta = 1$ and the $a^\dagger_{0,X}$ creates a spin coherent state with maximal spin length 3/2. In this limit, the $b_\pm$ branches correspond to magnons of the standard spin-wave theory and they are decoupled from the other modes. The $c_\pm$ and $d_\pm$ are local magnetic transitions with $\Delta S_W = 2$ and 3 corresponding to Zeeman energies $12J$ and $18J$, respectively, in the Weiss field $4 \times (3/2)J$ of the neighboring spins (S_W is the spin component parallel to the Weiss field). The $c_\pm$ and $d_\pm$ modes are generally silent in ESR, FIR, and INS spectra, as the magnetic dipolar matrix elements vanish in the imaginary part of the dynamic magnetic susceptibility, $\mathrm{Im}\chi^{mm}_{\alpha\alpha}(\omega) \propto \sum_f|\langle f|S^\alpha|\Psi_0\rangle|^2\delta(\omega - \omega_f + \omega_0)$. These transitions can only be excited by quadrupolar or higher order spin operators.

As we turn on $\Lambda > 0$, η increases and the spin length decreases in the Néel state [Eq. (2)]. The modes labeled as c_- and c_+ in Fig. 2 are spin-stretching modes, with

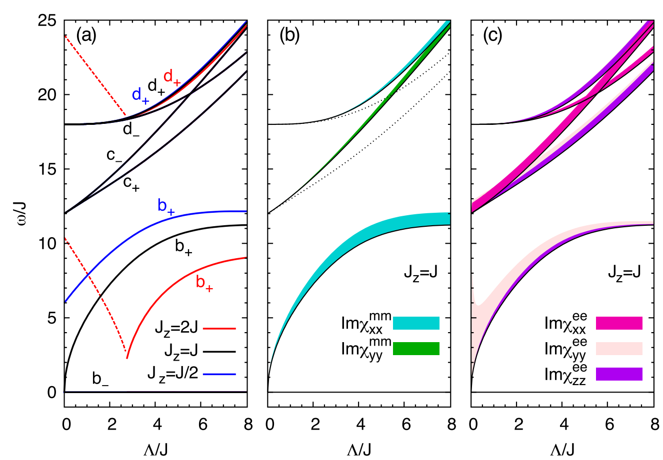

FIG. 2 (color online). (a) The energy of the modes for different values of J_z/J in zero field. b_- denotes the $\omega = 0$ Goldstone mode. Only the b_+ and d_+ modes depend on J_z/J. The dashed lines indicate modes in the easy-axis AF state that forms below $\Lambda \approx 2.7J$ for $J_z = 2$. (b) and (c) shows the imaginary part of the magnetic $\chi^{mm}_{\xi\xi}(\omega)$ and electric $\chi^{ee}_{\xi\xi}(\omega)$ dynamic susceptibilities, respectively, for $J = J_z$. The shading above the lines represent the strength of the magnetic and electric response.

spin length oscillating in and out of phase on the two sublattices, respectively. Hence, c_- is excited by the S^y spin operator, with a finite weight in $\mathrm{Im}\chi^{mm}_{yy}(\omega)$ that vanishes as $(\Lambda/J)^2$ when $\Lambda/J \to 0$. Most of the weight in $\mathrm{Im}\chi^{mm}_{xx}(\omega)$ comes from the low energy b_+ mode, while the contribution of d_+ to $\mathrm{Im}\chi^{mm}_{xx}(\omega)$ is $\propto (\Lambda/J)^4$, so that the sum rule $\int d\omega \mathrm{Im}\chi^{mm}_{xx}(\omega)/\omega = g^2_{xx}/8J$ is fulfilled. $\mathrm{Im}\chi^{mm}_{zz}(\omega)$ is zero for all but the Goldstone mode b_-.

For a large single-ion anisotropy ($\Lambda \gg J$, J_z), $\eta \propto \Lambda$ and the $S^z = \pm 3/2$ states are suppressed in the ground state, reducing the spin length from 3/2 to 1. We recover the spectra of isolated spins: two modes with energies $\omega/\Lambda \to 0$ and four with $\omega \to 2\Lambda$, in agreement with Ref. [11].

From the analysis of the dynamic magnetic susceptibility, it follows that some of these unconventional spin excitations (c_- and d_+ in the present case) become observable by ESR, FIR, and INS as soon as single-ion anisotropy gets significant. We expect such modes to appear in magnets with single-ion anisotropy irrespective of the details of their long range magnetic order and crystal structure.

Moreover, if the crystal lattice breaks the inversion symmetry, spin quadrupolar and electric dipole (or electric polarization) operators have the same symmetry properties. Thus a new channel opens to excite these modes as the electric field of the incident light can directly couple to the spin quadrupolar operators, allowing a response expressed by $\mathrm{Im}\chi^{ee}_{\alpha\alpha}(\omega)$ [11]. Indeed, d_- and c_+ modes with only magnetic quadrupol moment are excited this way and remain silent in $\mathrm{Im}\chi^{mm}_{\alpha\alpha}(\omega)$ irrespective of the Λ/J ratio. The dynamical electric susceptibility $\mathrm{Im}\chi^{ee}_{\alpha\alpha}(\omega)$ shows a strong response for most of the modes, as shown in Fig. 2(c). In general, noncentrosymmetric crystal structure can make the unconventional modes observable via electric dipole excitations even in magnets with no magnetic anisotropy.

Our calculation describes well the magnetic field dependence of the excitations in $Ba_2CoGe_2O_7$, see Fig. 1. From the fit of the experimental data we obtain $\Lambda = 13.4$ K, $J = 2.3$ K, $J_z = 1.8$ K, $g_{zz} = 2.1$ and $g_{xx} = g_{yy} = 2.3$. Magnetic field larger than 16 T in the easy plane is strong enough to drive a transition from a canted AF to an almost saturated magnet. This is observed as a kink in the 1 THz modes at $B_{\mathrm{dc}} \approx 16$ T [Fig. 1(b)]. The theory also predicts the onset of fully saturated phase for $B_{\mathrm{dc}} > 36$ T applied perpendicular to the easy plane (along the tetragonal axis), inducing a gap in the Goldstone mode [Fig. 1(a)], in agreement with Ref. [22]. The V-shape splitting of the 1 THz mode and the avoided crossing at $B_{\mathrm{dc}} \approx 12$ T for fields parallel to the tetragonal axis is also reproduced correctly [see Fig. 1(a) and 1(c)]. The lowest lying mode of the $f \sim 1$ THz branch is theoretically predicted to be weak [see dotted grey line in Fig. 2(b)] and does not appear in the experimental spectra. The only feature not explained by the model is the splitting of the $f \sim 0.5$ THz resonance above $B_{\mathrm{dc}} = 5$ T for fields perpendicular to the [001] axis.

The analytical solution of a pure spin Hamiltonian [see Eq. (1)] enabled us to fully characterize the excited states in terms of spin and polarization dynamics, implying that the electric polarization adiabatically follows the sublattice magnetization vector and does not have its "own" dynamics in the energy range of interest. The motion of the sublattice magnetization and the local polarization in zero field is visualized in Fig. 3 for the Goldstone mode and for a spin-stretching mode. The Goldstone mode is associated with the oscillation of the polarization along the tetragonal axis and has a direct connection with the dc magnetoelectric effect. The spin-stretching mode shows more complex polarization dynamics (see Supplemental Material [17]), for example, for $\Lambda \to 0$ the polarization still oscillates even though the magnetic moment is frozen.

Our theory describes the unconventional spin-wave excitations in $Ba_2CoGe_2O_7$ and provides a guide for spin-wave spectroscopy in a broad class of ordered magnets with strong magnetic anisotropy and/or a noncentrosymmetric lattice structure. We expect unconventional spin excitations to emerge in the dynamic magnetic susceptibility whenever a large single-ion anisotropy is present in a $S > 1/2$ system. Moreover, if the inversion symmetry of the crystal is broken, these new modes can have a dielectric response even in isotropic magnets. The combined effect of broken inversion and magnetic anisotropy is particularly efficient to make these unconventional modes observable. They should be detected by THz light absorption or

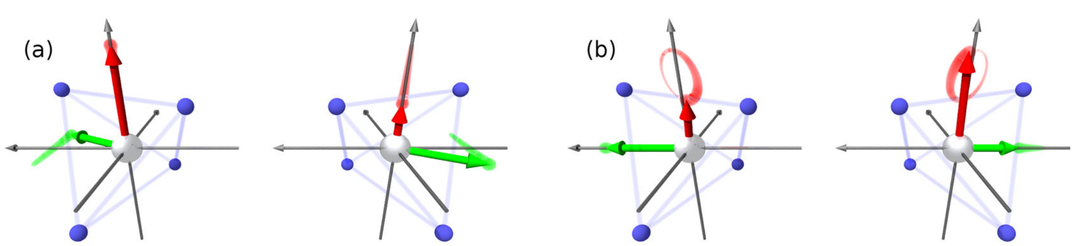

FIG. 3 (color online). Motion of the magnetizations (green, light arrows) and the local electric polarizations (red, dark arrows) in the two sublattices (a) for the Goldstone mode (b_- in Fig. 2) and (b) for the c_- stretching mode. The blue spheres are the oxygens forming tetrahedral cages around the central Co ions. The vertical axis is the tetragonal one, while the horizontal axes point along [110] and $[1\bar{1}0]$. Apparent tilting of the axes comes from the perspective view.

inelastic neutron scattering via the induced magnetic and/or electric dipole moment.

We are grateful for stimulating discussions with S. Miyahara, N. Furukawa, N. Kida, Y. Onose, and B. Náfrádi. This work was supported by Hungarian OTKA under Grant Nos. PD75615, CNK80991, K73361, K73455, K107228, and NN76727, Bolyai program, TÁMOP-4.2.2.B-10/1–2010-0009, by EuroMAgNET II under the EU Contract No. 228043, by Estonian Ministry of Education and Research Grant No. SF0690029s09, Estonian Science Foundation Grant Nos. ETF8170 and ETF8703, and the bilateral program of the Estonian and Hungarian Academies of Sciences.

Note added in proof.—Professor M. Matsumoto kindly informed the authors that the possibility to observe spin-stretching (''longitudinal'') modes in spin systems with single-ion anisotropy by INS and Raman scattering was also discussed in Refs. [23,24].

[1] J. Van Kranendonk and J. H. Van Vleck, Rev. Mod. Phys. **30**, 1 (1958).
[2] E. Turov, *Physical Properties of Magnetically Ordered Crystals* (Academic, New York, 1965).
[3] R. Shiina, H. Shiba, P. Thalmeier, A. Takahashi, and O. Sakai, J. Phys. Soc. Jpn. **72**, 1216 (2003).
[4] S. Carretta, P. Santini, R. Caciuffo, and G. Amoretti, Phys. Rev. Lett. **105**, 167201 (2010).
[5] I. Kézsmárki, N. Kida, H. Murakawa, S. Bordács, Y. Onose, and Y. Tokura, Phys. Rev. Lett. **106**, 057403 (2011).
[6] C. de la Cruz (private communication).
[7] A. Zheludev, T. Sato, T. Masuda, K. Uchinokura, G. Shirane, and B. Roessli, Phys. Rev. B **68**, 024428 (2003).
[8] H. Murakawa, Y. Onose, S. Miyahara, N. Furukawa, and Y. Tokura, Phys. Rev. Lett. **105**, 137202 (2010).
[9] H. T. Yi, Y. J. Choi, S. Lee, and S.-W. Cheong, Appl. Phys. Lett. **92**, 212904 (2008).
[10] S. Bordacs, I. Kezsmarki, D. Szaller, L. Demko, N. Kida, H. Murakawa, Y. Onose, R. Shimano, T. Room, U. Nagel, S. Miyahara, N. Furukawa, and Y. Tokura, arXiv:1109.1597.
[11] S. Miyahara and N. Furukawa, J. Phys. Soc. Jpn. **80**, 073708 (2011).
[12] P. Toledano, D. D. Khalyavin, and L. C. Chapon, Phys. Rev. B **84**, 094421 (2011).
[13] K. Yamauchi, P. Barone, and S. Picozzi, Phys. Rev. B **84**, 165137 (2011).
[14] M. Akaki, J. Tozawa, D. Akahoshi, and H. Kuwahara, Appl. Phys. Lett. **94**, 212904 (2009);M. Akaki, J. Tozawa, M. Hitomi, D. Akahoshi, and H. Kuwahara, J. Phys.: Conf. Ser. **200**, 012003 (2010).
[15] H. Murakawa (private communication).
[16] J. Romhányi, F. Pollmann, and K. Penc, Phys. Rev. B **84**, 184427 (2011); J. Romhányi, M. Lajkó, and K. Penc, Phys. Rev. B **84**, 224419 (2011).
[17] See Supplemental Material at http://link.aps.org/supplemental/10.1103/PhysRevLett.108.257203 for the exact form of the transformed Hamiltonian, the details of the calculation, and for an animated representation of each mode.
[18] A. Joshi, M. Ma, F. Mila, D. N. Shi, and F. C. Zhang, Phys. Rev. B **60**, 6584 (1999).
[19] M. Matsumoto, B. Normand, T. M. Rice, and M. Sigrist, Phys. Rev. B **69**, 054423 (2004).
[20] N. Papanicolaou, Nucl. Phys. **B240**, 281 (1984); **B305**, 367 (1988).
[21] F. Onufrieva, Zh. Eksp. Teor. Fiz. **89**, 2270 (1985) [Sov. Phys. JETP **62**, 1311 (1985)]; A. V. Chubukov, J. Phys. Condens. Matter **2**, 1593 (1990).
[22] J. W. Kim, S. H. Khim, S. H. Chun, K. H. Kim, E. Choi, Y. Jo, L. Balicas, N. Harrison, H. Yi, S.-W. Cheong, J. H. Han, and C. D. Batista, in National High Magnetic Field Laboratory Annual Report, 2010, ''Investigation of a Quantum Critical Point in Multiferroic $Ba_2CoGe_2O_7$,'' p. 20.
[23] M. Matsumoto and M. Koga, J. Phys. Soc. Jpn. **76**, 073709 (2007).
[24] M. Matsumoto, H. Kuroe, T. Sekine, and T. Masuda, J. Phys. Soc. Jpn. **79**, 084703 (2010).